Human Molecular Genetics, 2009, Vol. 18, No. 1 ***118–127***
doi:10.1093/hmg/ddn322
Advance Access published on October 4, 2008

Transcript- and tissue-specific imprinting of a tumour suppressor gene

Reiner Schulz[1], Ruth B. McCole[1], Kathryn Woodfine[1,†], Andrew J. Wood[1,‡], Mandeep Chahal[1], David Monk[2], Gudrun E. Moore[2] and Rebecca J. Oakey[1,*]

[1]Department of Medical and Molecular Genetics, King's College London, London SE1 9RT, UK and [2]Clinical and Molecular Genetics, Institute of Child Health, University College London, London WC1N 1EH, UK

Received June 25, 2008; Revised September 21, 2008; Accepted October 2, 2008

The Bladder Cancer-Associated Protein gene (*BLCAP*; previously *BC10*) is a tumour suppressor that limits cell proliferation and stimulates apoptosis. *BLCAP* protein or message are downregulated or absent in a variety of human cancers. In mouse and human, the first intron of *Blcap/BLCAP* contains the distinct Neuronatin (*Nnat/NNAT)* gene. *Nnat* is an imprinted gene that is exclusively expressed from the paternally inherited allele. Previous studies found no evidence for imprinting of *Blcap* in mouse or human. Here we show that *Blcap* is imprinted in mouse and human brain, but not in other mouse tissues. Moreover, *Blcap* produces multiple distinct transcripts that exhibit reciprocal allele-specific expression in both mouse and human. We propose that the tissue-specific imprinting of *Blcap* is due to the particularly high transcriptional activity of *Nnat* in brain, as has been suggested previously for the similarly organized and imprinted murine *Commd1/U2af1-rs1* locus. For *Commd1/U2af1-rs1*, we show that it too produces distinct transcript variants with reciprocal allele-specific expression. The imprinted expression of *BLCAP* and its interplay with *NNAT* at the transcriptional level may be relevant to human carcinogenesis.

INTRODUCTION

The Bladder Cancer-Associated Protein gene (*BLCAP*; previously *BC10*) was first identified in a differential gene expression study where it was found to be specifically silenced in invasive human bladder transitional cell carcinoma (1). Loss of *BLCAP* expression has since also been observed in renal-cell carcinoma (2) and cervical cancer (3). Overexpression of BLCAP in HeLa and human tongue carcinoma cells stimulates apoptosis (3,4). Relative to other tissues, the Novartis gene expression atlas (SymAtlas) shows *BLCAP* mRNA levels to be high in brain, the pituitary and the immune system (5) (Affymetrix probe set 201032_at).

BLCAP is translated in *vitro* into a ~9.8 kDa protein of 87 amino acids whose function is unknown but which putatively includes two *trans*-membrane domains, cytoplasmic domains at the N and C terminals, a phosphorylation site and may bind DNA (6) (UniProt/SwissProt: P62952). At the amino acid level, BLCAP is identical in human, mouse (P62951), orangutan (Q5R692), rat (P62950), cat (P62953) and cattle (P62954).

Human *BLCAP* is located on Chr 20q11.2 and is annotated in RefSeq (NM_006698) as having two exons, with the open reading frame confined to the last exon. An exceptional feature of the locus is the existence of a distinct gene, Neuronatin (*NNAT*), within the intron of *BLCAP*. Distinct CpG islands (CGI) overlap the transcription start sites (TSSs) of both *NNAT* and *BLCAP*, with an additional CGI in the body of *NNAT*. *NNAT* is imprinted and paternally expressed in fetal brain (7). The same study found ~50% of CpGs in a region encompassing the *NNAT* CGIs to be methylated in brain and other tissues, suggestive of differential, maternal allele-specific methylation. However, no evidence was found for imprinted expression of *BLCAP* in fetal brain or other tissues, and the *BLCAP* CGI was unmethylated in all investigated tissues (7).

*To whom correspondence should be addressed at: Department of Medical and Molecular Genetics, King's College London, Guy's Campus, Guy's Hospital, 8th floor Tower Wing, London SE1 9RT, UK. Tel: +44 207188 3711; Fax: +44 2071882585; Email: rebecca.oakey@genetics.kcl.ac.uk
†Present address: Cancer Research UK Cambridge Research Institute, Cambridge University, Cambridge CB2 0RE, UK.
‡Present address: Department of Molecular and Cell Biology, University of California at Berkeley, CA 94720-3204, USA.

The orthologous murine *Blcap/Nnat* locus on Chr 2 largely recapitulates the genomic organization and expression profile of human *BLCAP/NNAT*. The intron harbours *Nnat* whose imprinting and paternal-specific expression was first observed in mouse embryo and newborn brain (8). *Blcap* mRNA levels are relatively high in brain and the pituitary, but not the immune system (SymAtlas probe set gnf1m03525_a_at). In addition, *Blcap* expression is high in adipose tissue, oocytes and zygotes, for which SymAtlas contains no human data. The promoters of *Nnat* and *Blcap* are associated with CGIs that are smaller than in human. In embryos, the *Nnat* CGI and gene body are methylated only on the maternal allele (9). The *Blcap* CGI is unmethylated, and expression assays in androgenetic, parthenogenetic and uniparentally disomic embryos suggested that *Blcap* is not imprinted (10).

Here, we show that murine and human *Blcap* generate multiple transcripts that are imprinted in the brain where expression occurs preferentially from either the maternal or the paternal allele in a transcript-specific manner. For the mouse, we quantify the relative contributions of representative transcripts to the mRNA pool and demonstrate that the regulation of the locus depends on maternal germline methylation. We argue that past studies found no evidence of *Blcap* imprinting due to the tissue-specific nature of *Blcap* imprinting (7,10). We compare the locus with other imprinted domains where the gene carrying the primary imprint mark is located in the intron of a gene that also exhibits parent-of-origin-specific expression (11,12). Based on similarities with these other loci, we propose that the high level of *Nnat* transcription in brain relative to other tissues contributes to the brain-specific imprinted expression pattern of *Blcap*. Our findings shed new light on the epigenetic regulation of a tumour suppressor gene and have implications for its deregulation during carcinogenesis.

RESULTS

Multiple *Blcap* transcripts are generated from distinct promoters in human and mouse

Several mouse (e.g. CJ174807) and human expressed sequence tags (ESTs; e.g. DA770824, DA366527, DA277117) suggested that additional *Blcap* TSSs exist in both species. In human, ESTs also indicated an alternatively spliced third internal *BLCAP* exon overlapping the *NNAT* coding sequence (e.g. DA377434). We have identified at least four distinct human and two distinct mouse *Blcap* transcripts (Fig. 1). They fall into two categories, depending on whether their TSSs are downstream or upstream of *Nnat*. We refer to *Blcap* transcripts with TSSs downstream of *Nnat* collectively as *Blcap_v1* and denote specific transcripts with a one letter suffix. Analogously, *Blcap_v2* stands for isoforms with TSSs upstream of *Nnat*.

Microarray measurements suggest preferential maternal expression of murine *Blcap*

We measured gene expression in whole head samples of newborn mice with maternal and paternal uniparental duplication (UpDp) of distal Chr 2 (13), which includes the *Blcap* locus. Thus, both homologous copies of the *Blcap* locus are of either the maternal or the paternal epigenotype. Two microarrays containing probe sets specific to *Blcap* and *Nnat* (Fig. 1B) were hybridized with a MatDp(dist2) sample and a PatDp(dist2) sample, respectively. The *Blcap* probe set detected ~2.4-fold more *Blcap* expression in MatDp(dist2) than in PatDp(dist2) material. The *Nnat* probe set, as expected, essentially failed to detect *Nnat* message in the MatDp(dist2) sample, while registering high *Nnat* levels in PatDp(dist2) newborn head (MatDp(dist2)/PatDp(dist2) = ~0.006).

SNP-based allele-specific direct sequencing and quantitative real-time PCR confirm preferential maternal expression of *Blcap_v1a* in mouse brain

A T/A SNP between the C57BL/6J (B6) and *Mus mus castaneus* (cast) mouse strains was identified in the last *Blcap* exon (Fig. 1B). It was used to determine the allelic origin of *Blcap_v1a* expression in newborn and adult brain samples of B6 × cast (B × C) and cast × B6 (C × B) inter-subspecific hybrid offspring. *Blcap_v1a* was specifically amplified from cDNA and directly sequenced. The maternal allele always dominated the sequencing traces, consistent with preferential maternal expression of *Blcap_v1a* (Fig. 2A). For further confirmation and to more accurately quantify the contribution of the parental alleles, we measured *Blcap_v1a* expression in MatDp(dist2) and PatDp(dist2) newborn brain samples relative to a matched non-UpDp control sample by TaqMan quantitative real-time PCR (qRT–PCR). We observed ~2.2-fold more *Blcap_v1a* expression in MatDp(dist2) than in the control, while PatDp(dist2) brain retained ~25% of the expression level in the control (Fig. 3A). This corresponds to ~8.8-fold more *Blcap_v1a* transcript in MatDp(dist2) than in PatDp(dist2) brain, a larger fold-change than observed via microarray in whole head samples.

Preferential maternal *Blcap_v1a* expression is present in embryo, but not in placenta or adult murine tissues other than brain

A second, G/C SNP between B6 and cast (Fig. 1B) was used for allele-specific sequencing assays of cDNA derived from whole embryo at 9.5 days post coitum (dpc), 13.5 dpc placenta and testis, heart, lung, liver and skeletal muscle tissue of adult mice. Preferential maternal *Blcap_v1a* expression was only observed in embryo (Fig. 2B and Supplementary Material, Fig. S1), likely due to the brain component of this RNA sample. Biallelic expression of *Blcap_v1a* in tissues other than brain likely contributed to the reduced fold-change observed via microarray in whole head samples in comparison to the brain samples assayed by qRT–PCR.

Blcap_v2a originating upstream of *Nnat* is, like *Nnat*, only expressed from the paternal allele

EST evidence for an alternative *Blcap* TSS upstream of the *Nnat* promoter prompted us to determine whether this transcript isoform was imprinted (*Blcap_v2a* in Fig. 1B). We amplified a product with intron boundaries identical to EST CJ174807 including almost the entire length of the last

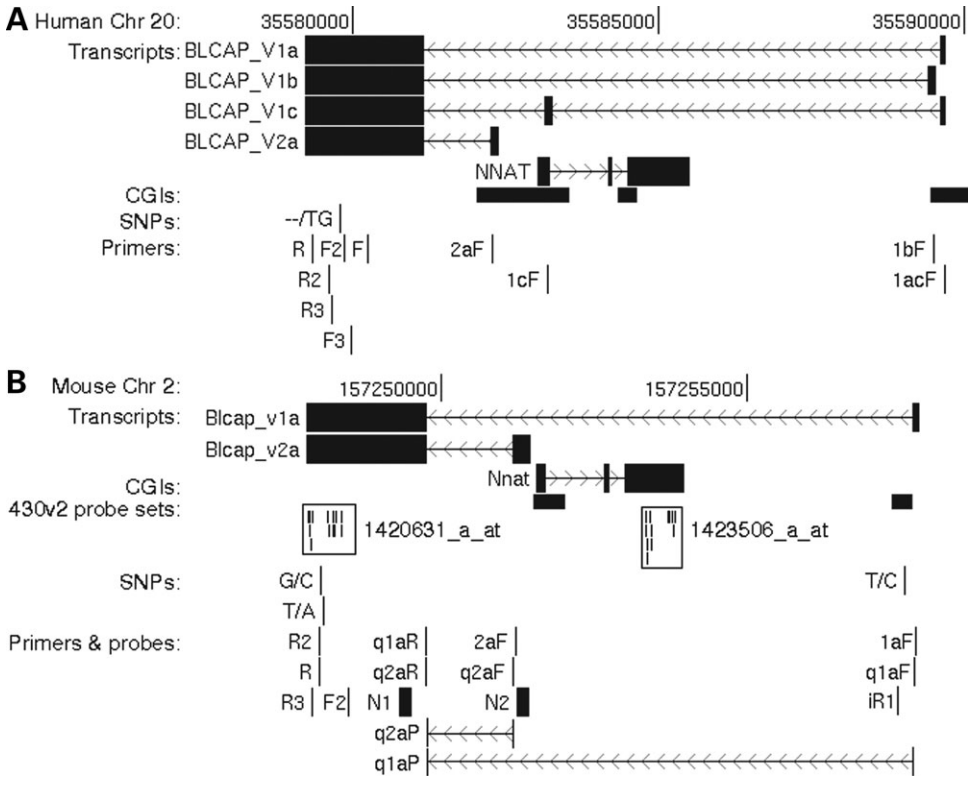

Figure 1. Genomic organization and features of the human *BLCAP* (**A**) and murine *Blcap* (**B**) loci. Each panel shows a base pair scale, the likely exon–intron structure of transcripts and the positions of CpG islands (CGIs), single nucleotide polymorphisms (SNPs) and PCR primers referred to in the text. Base pair coordinates are with respect to the human Mar 2006 v36.1 and the mouse Feb 2006 v36.0 NCBI genome builds. (A) and (B) are drawn to the same scale, each displaying a genomic region of ~13 kb. Transcript structures were inferred from ESTs and the results of the PCR, sequencing and northern blot experiments described in the text. Transcripts are shown with filled boxes delineating exons and thin lines with chevrons denoting introns and direction of transcription. (B) also displays the locations of mouse expression microarray (Affymetrix 430v2), TaqMan quantitative real-time PCR and northern probes. The TaqMan probes are intron-spanning, as indicated. Microarray probes are displayed as small vertical lines, and a frame indicates the probes belonging to the same probe set. Primer and probe sequences, and experimental conditions are listed in Supplementary Material, Table S1. The figure was generated with the UCSC genome browser (40).

Blcap exon. Sequencing showed that in newborn brain and whole embryo, *Blcap_v2a* was exclusively expressed from the paternal allele (Fig. 2C). This was confirmed by TaqMan qRT–PCR: amplification failed in MatDp(dist2) newborn brain due to a lack of *Blcap_v2a* transcripts, while an approximately 2-fold increase of *Blcap_v2a* was observed in PatDp(dist2) newborn brain relative to the non-UpDp control (Fig. 3A).

Since the microarray probe set for *Blcap* is located in the last exon that is shared by *Blcap_v1a* and *Blcap_v2a*, the microarray measurements likely reflect the cumulative levels of both isoforms. Nevertheless, the microarray detected a ~2.4-fold change in MatDp(dist2) relative to PatDp(dist2), suggesting that the paternally expressed *Blcap_v2a* is much less abundant than the predominantly maternally expressed *Blcap_v1a*. Based on our previous qRT–PCR measurements in newborn brain, *Blcap_v1a* is ~100-fold more abundant than *Blcap_v2a* (Fig. 3B). Hence, *Blcap_v2a* is unlikely to have significantly contributed to the microarray measurements so that the small MatDp(dist2)/PatDp(dist2) ratio in relation to the qRT–PCR results is most likely due to the brain-specific imprinting of *Blcap*.

Transcript analysis by northern hybridization confirms findings for *Blcap_v1a* and *Blcap_v2a*

Two northern blots with newborn brain RNA of MatDp(dist2), PatDp(dist2) and non-UpDp mice were hybridized with a probe to the last *Blcap* exon and a probe to the first exon of *Blcap_v2a*. The former generated a single band in all three lanes (Fig. 4), which corresponds to the known size of *Blcap_v1a* (2079 bp), the more abundant of the two *Blcap* transcripts. The lack of additional distinct bands is evidence for the absence of additional major *Blcap* transcripts. However, the last *Blcap* exon contributes >87% to the length of the two known transcripts so that additional transcripts with small alternative first exons may have been subsumed in the one band. The band was most intense in the MatDp(dist2) and least intense in the PatDp(dist2) lane, even though the RNA load of the PatDp(dist2) lane was higher (Fig. 4). This indicates that in newborn brain, transcripts sharing the last *Blcap* exon cumulatively originate most often from the maternal allele, consistent with the microarray measurements in whole newborn head.

The probe specific for *Blcap_v2a* generated an obvious band in only the PatDp(dist2) lane at a position consistent

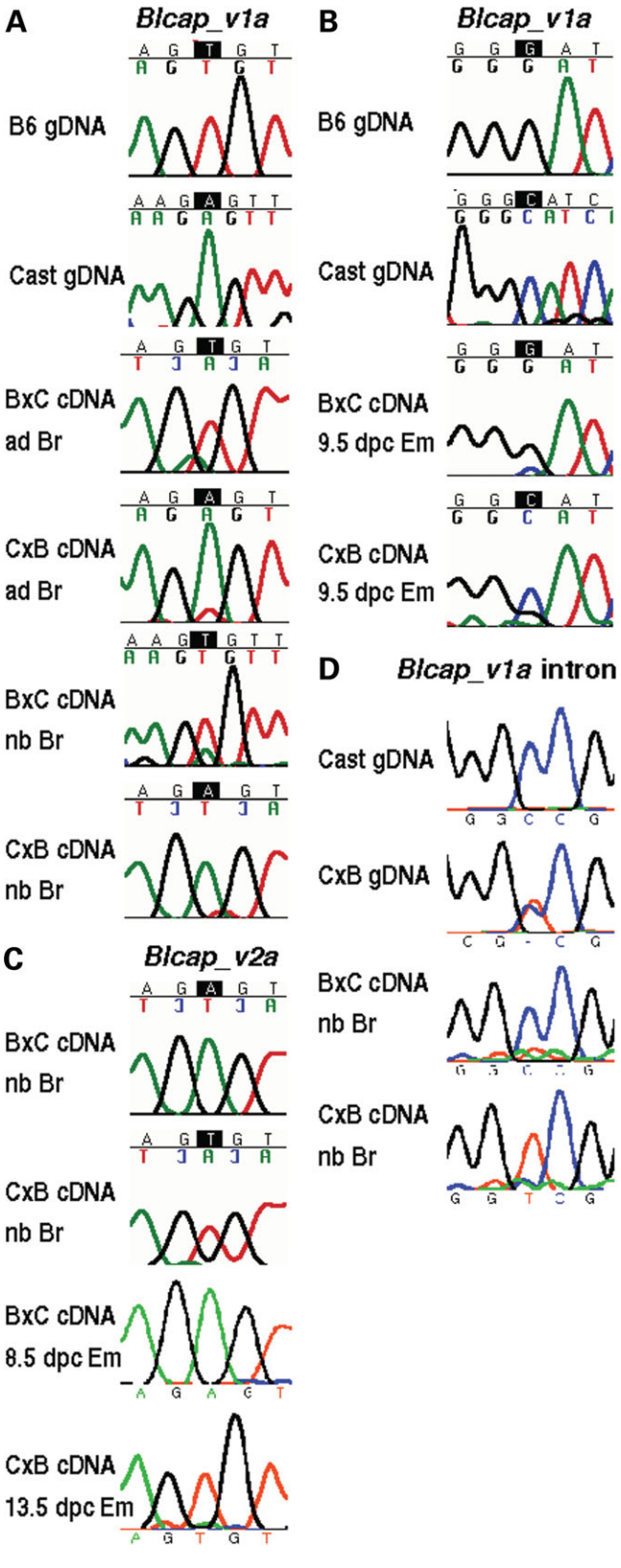

with the slightly larger size of *Blcap_v2a* (2258 bp) relative to *Blcap_v1a*. At the same position, a very faint band could be seen in the non-UpDp lane, but there was no signal in the MatDp(dist2) lane, indicating paternal-only expression.

Blcap expression is regulated by maternal germline methylation

In the mouse, the DNA methyltransferase 3-like (*Dnmt3l*) protein is required during oogenesis to establish the maternal-specific methylation marks that in the offspring, control the parent-of-origin-specific expression of most imprinted genes (14,15). In $Dnmt3l^{-/+}$ offspring of $Dnmt3l^{-/-}$ dams and wild-type sires, the imprinting control regions (ICRs) that normally carry a maternal methylation mark are unmethylated on both alleles, leading to the misregulation of developmentally crucial imprinted genes and death by 9.5 dpc (14). Our previous microarray measurements of gene expression in $Dnmt3l^{-/+}$ 8.5 dpc embryos versus wild-type litter mates showed a decrease of *Blcap* expression to ~70% of wild-type levels and an increase in *Nnat* expression by ~40% (16). Measurements of *Blcap_v1a* and *Blcap_v2a* by qRT–PCR showed a reduction of *Blcap_v1a* in $Dnmt3l^{-/+}$ embryos to ~50% of wild-type levels, whereas *Blcap_v2a* levels increased by ~40% (Fig. 3C).

In embryo, the *Nnat* promoter (including a *Bss*HII restriction site ~50 bp upstream of the TSS) and gene body were previously shown to be methylated on only the maternal allele (9). In human, differential methylation of *NNAT* has been observed even farther upstream, to within the last exon of *BLCAP* (7). The above changes in *Blcap* expression levels in $Dnmt3l^{-/+}$ embryos are consistent with the notion that this methylation mark is established during oogenesis and that in the offspring, it acts as the ICR of the *Blcap* locus. To investigate this further, we performed a bisulfite mutagenesis methylation assay of the *Blcap_v2a* and *Nnat*

Figure 2. Allele-specific sequencing results for murine *Blcap*. (**A**) The two top-most rows of sequencing traces labelled gDNA (genomic DNA) show the B6 (T) and cast (A) genotypes at the site of the T/A SNP between the two strains (Fig. 1B). The other rows contain the traces obtained from amplifying and sequencing *Blcap_v1a* using adult (ad) and newborn (nb) brain (Br) cDNA samples of B6 × cast (B × C) and cast × B6 (C × B) inter-subspecific hybrids (denoted in dam × sire order). In both adult and newborn brain and for both directions of the cross, the dominant peak in the trace at the site of the SNP corresponds to the maternal allele, indicating *Blcap_v1a* expression from preferentially the maternal allele. (**B**) A G/C SNP between B6 and cast (top gDNA traces and Fig. 1B) was used to determine the allelic origin of *Blcap_v1a* expression in 9.5 dpc embryo (Em). The maternal allele dominated the sequence traces for the B × C and C × B hybrid embryo samples, indicating preferential maternal expression. (**C**) The same T/A SNP as in (A) was used to test for allele-specific expression of *Blcap_v2a* (Fig. 1B). In B × C and C × B newborn brain and whole embryo, *Blcap_v2a* was expressed from exclusively the paternal allele, in contrast to *Blcap_v1a*. (**D**) Allele-specific sequencing of transcripts in the first intron of *Blcap_v1a* using a T/C SNP between the B6 and cast strains (top gDNA traces and Fig. 1B). Transcripts amplified from B × C and C × B newborn (nb) brain (Br) were predominantly expressed from the paternal allele.

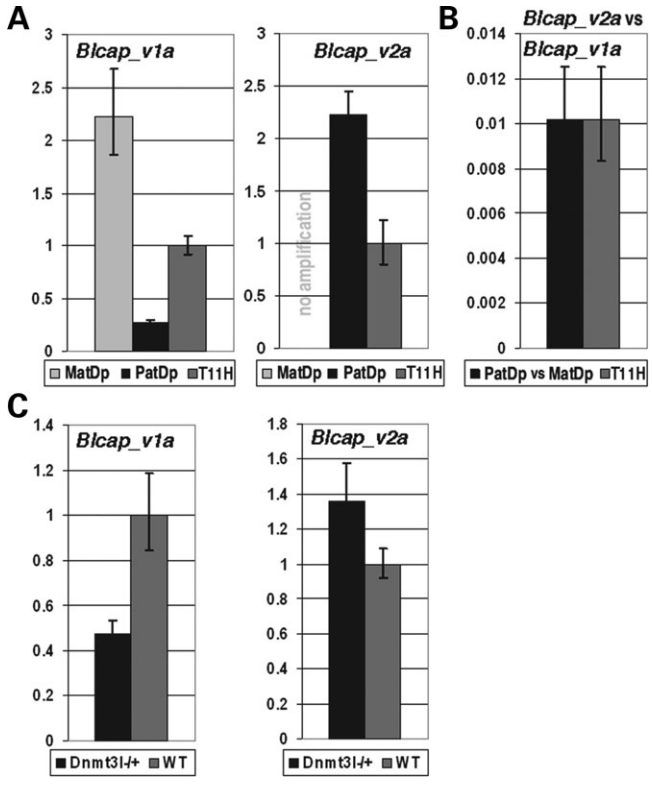

Figure 3. TaqMan quantitative real-time PCR (qRT–PCR) measurements of *Blcap_v1a* and *Blcap_v2a*. Error bars indicate the 95% confidence interval. (**A**) *Blcap_v1a* and *Blcap_v2a* levels in MatDp(dist2) and PatDp(dist2) newborn (nb) brain relative to a matched non-UpDp control (T11H). *Blcap_v1a* was ∼2.2 times more abundant in MatDp(dist2) than in control nb brain, and achieved only ∼25% of the control expression level in PatDp(dist2) nb brain, which corresponds to a MatDp(dist2)/PatDp(dist2) expression ratio of ∼8.8. This reflects the preferential maternal expression of *Blcap_v1a. Blcap_v2a* was not present in MatDp(dist2) nb brain (no amplification), and ∼2-fold more abundant in PatDp(dist2) than in non-UpDp nb brain, consistent with paternal-only expression. (**B**) Left bar: amount of *Blcap_v2a* in PatDp(dist2) nb brain relative to *Blcap_v1a* in MatDp(dist2) nb brain. Right bar: amount of *Blcap_v2a* in non-UpDp nb brain relative to *Blcap_v1a* in the same sample. In both cases, *Blcap_v2a* reached only ∼1% of the *Blcap_v1a* transcript level, i.e. in nb brain, *Blcap_v1a* is ∼100-fold more abundant than *Blcap_v2a*. (**C**) Quantification of *Blcap_v1a* and *Blcap_v2a* levels in 8.5 dpc $Dnmt3l^{-/+}$ embryos relative to wild-type (WT) litter-mates. Expression of *Blcap_v1a* was reduced to ∼50% of WT level in $Dnmt3l^{-/+}$ embryos, while *Blcap_v2a* increased in abundance by ∼40%. This is consistent with the notion that the maternal allele-specific methylation of the *Nnat* promoter CGI is established during oogenesis and that methylation of this CGI positively regulates *Blcap_v1a* expression, while it inhibits *Blcap_v2a* expression.

promoter region (Supplementary Material, Fig. S2). Overall, we observed a loss of methylation in $Dnmt3l^{-/+}$ relative to wild-type samples across the entire region, suggesting that its methylation significantly depends on the activity of *Dnmt3l* during oogenesis.

Human orthologues of *Blcap_v1a* and *Blcap_v2a* are imprinted in fetal brain

The genomic organization of the human *BLCAP* locus is similar to murine *Blcap*, including alternative *BLCAP* isoforms (Fig. 1A). *BLCAP_V1a*, *b* and *c* are orthologous to

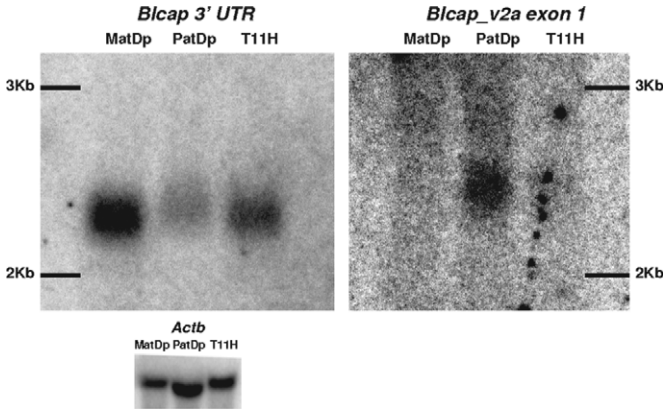

Figure 4. Detection of *Blcap_v1a* and *Blcap_v2a* in MatDp(dist2), PatDp(-dist2) and non-UpDp (T11H) newborn brain RNA by northern hybridization. The signal obtained with an *Actb* probe is shown as a loading control (bottom). Left: Hybridization signal produced by the probe designed to the last Blcap exon (N1 in Fig. 1B). A single band was observed in all three lanes where the relative band intensity was highest in the MatDp(dist2) lane and lowest in the PatDp(dist2) lane. Band position and relative intensities were consistent with the known size of the major *Blcap* transcript *Blcap_v1a* (2079 bp) and overall preferential expression of *Blcap* from the maternal allele in newborn brain. Right: Results obtained with a probe specific to the first exon of *Blcap_v2a* (N2 in Fig. 1B). No band was present in the MatDp(dist2) lane. A single band was visible in the PatDp(dist2) lane. At the corresponding position in the non-UpDp lane, a very faint band was present. This indicates paternal-only expression of *Blcap_v2a*. The band was slightly shifted upward relative to the band obtained with the N1 probe, as is expected of the slightly larger *Blcap_v2a* (2258 bp). The exposure times necessary to visualize the results for *Blcap_v2a* were considerably longer than for the N1 probe, which is consistent with the low abundance of *Blcap_v2a* relative to *Blcap_v1a* as determined by qRT–PCR.

Blcap_v1a in the sense that their TSSs are downstream of *NNAT*. Analogously, *BLCAP_V2a* upstream of *NNAT* is orthologous to *Blcap_v2a*. To determine whether this similarity extends to the imprinting status of these *BLCAP* isoforms, we performed allele-specific sequencing assays in brain samples of human fetuses that were heterozygous for a TG_n repeat copy number polymorphism (rs_11474161) in the last *BLCAP* exon where $n = 7$ or $n = 8$, i.e., n differed between the parental alleles by one.

In fetus no. 1, *BLCAP_V1a, b* and *c* were predominantly expressed from the $n = 7$ allele, while *BLCAP_V2a* transcripts originated from the $n = 8$ allele, indicating reciprocal allele-specific expression (Fig. 5). Primers designed to the last *BLCAP* exon, thought to be shared by all isoforms, amplified only the $n = 7$ allele, suggesting that the *BLCAP_V1* isoforms transcribed from the $n = 7$ allele are overall more abundant than isoforms like *BLCAP_V2a* that are expressed from the $n = 8$ allele. This recapitulates our observations on the relative expression levels of *Blcap_v1a* and *Blcap_v2a* in the mouse. For fetus no. 1, no parental sample was available, precluding parent-of-origin determination. For a second fetus (no. 2), maternal genomic DNA (gDNA) was available and the maternal genotype was $n = 7$ (Fig. 5). Predominantly the maternal $n = 7$ allele of *BLCAP_V1a, b* and *c* was present in brain cDNA of fetus no. 2, as opposed to *BLCAP_V2a* which originated exclusively from the paternal $n = 8$ allele (Fig. 5). These data indicate that the parent-of-origin-specific expression profile of murine *Blcap* is conserved in human,

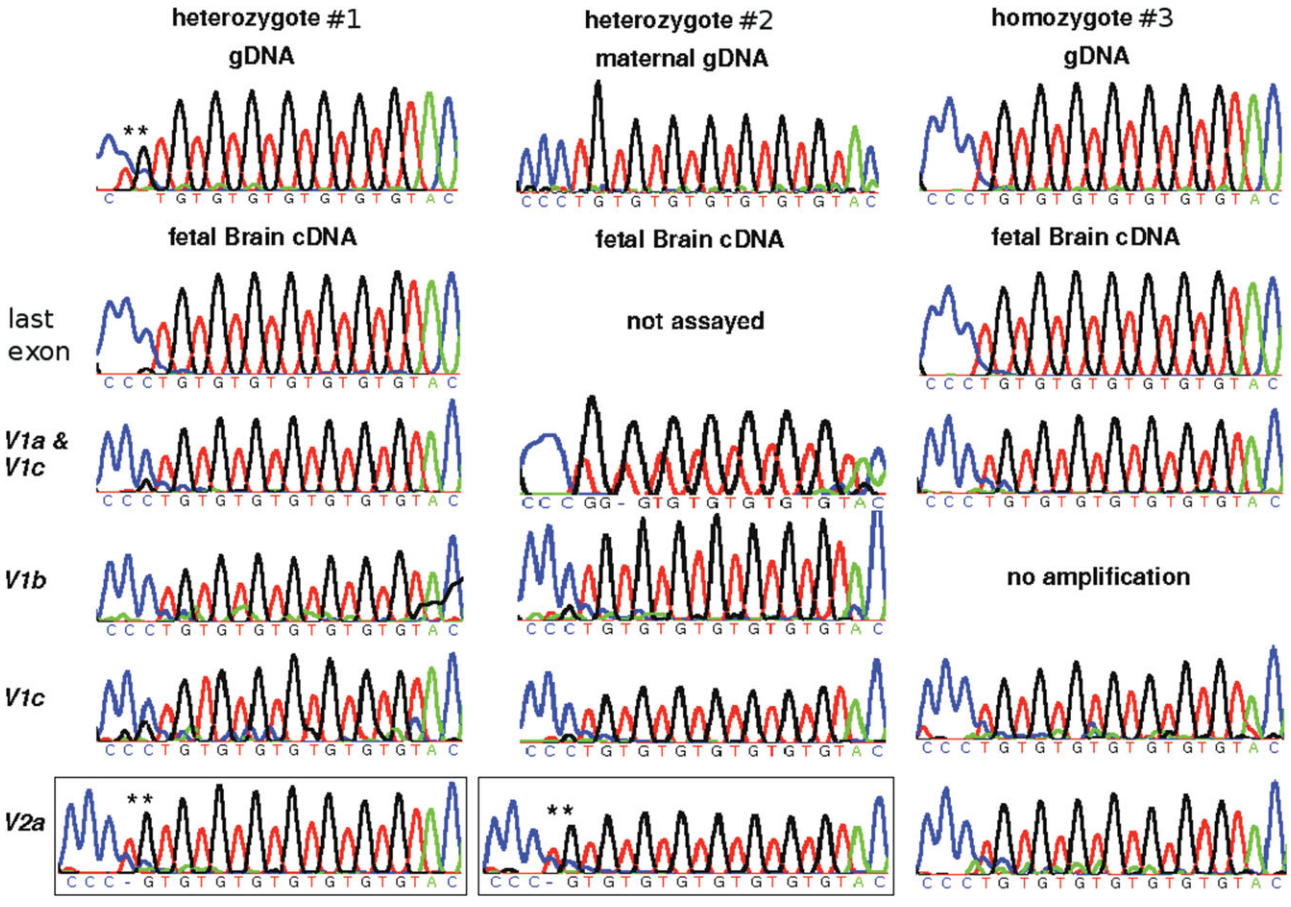

Figure 5. Human allele-specific sequencing results. For each fetus, the top row contains a trace generated from genomic DNA (gDNA). For fetus no. 1 (left), this trace demonstrates heterozygosity for a TG_n repeat copy number polymorphism in the last *BLCAP* exon ($n = 7$ for one allele, and $n = 8$ for the other; asterisks highlight the additional TG dinucleotide). For fetus no. 2 (middle), the maternal gDNA trace shows the maternal genotype to be $n = 7$. The second and subsequent rows display traces obtained with fetal brain cDNA. In fetus no. 1, only the $n = 7$ allele is evident after sequencing of PCR products generated with primers designed to the last *BLCAP* exon, thought to be common to all *BLCAP* isoforms. Similar results were observed for amplicons specific to isoforms *BLCAP_V1a* and *c, BLCAP_V1b* and *BLCAP_V1c*. This was also the case for fetus no. 2. In contrast, the $n = 8$ allele was seen upon sequencing *BLCAP_V2a* products in both fetuses nos 1 and 2 (framed traces; asterisks highlight the additional TG). These data indicate that *BLCAP_V2a* is predominantly expressed from the paternal allele, while the other isoforms are preferentially expressed from the maternal allele. For comparison, an $n = 7$ homozygous fetus (no. 3) is shown on the right.

including the relatively minor contribution of paternal transcripts like *BLCAP_V2a* to the overall *BLCAP* transcript pool.

Paternal allele-specific transcripts extending into the first intron of *Blcap_v1a*

The first intron of *Blcap_v1a* prior to *Nnat* contains three AATAAA polyadenylation (polyA) site motifs in the sense orientation relative to *Blcap*. Two of them are only 25 bp apart, are located within a ~60 bp region that is evolutionarily conserved among mammals, and coincide with the ends of multiple ESTs and an mRNA that likely correspond to *Blcap* transcripts (BY664891, CJ320720, AV349270, BB178170, AK038884). However, they may also correspond to anti-sense transcripts generated by *Nnat*. All these transcripts were recovered from brain tissues or Rathke's pouch, an embryonic precursor of parts of the pituitary.

Allele-specific sequencing assays were performed using a T/C SNP between B6 and cast near the start of the *Blcap_v1a* intron (Fig. 1B). Multiple, differentially spliced transcripts were amplified from newborn brain. Sequencing of amplicons that covered the SNP position and whose parental origin could thus be determined, revealed that they originated from the paternal allele (Fig. 2D).

The *Commd1/U2af1-rs1* locus generates paternal allele-specific transcripts similar to *Blcap_v2a*

The murine *Commd1* (=*Murr1*)*/U2af1-rs1* locus on proximal Chr 11 has been noted previously as being similar in organization to *Blcap*/*Nnat* (11). In previous microarray experiments, we compared MatDp(prox11) with PatDp(prox11) tissues, including brain (17). For *Commd1/U2af1-rs1*, these microarray measurements reflected the known preferential maternal expression of *Commd1* and the paternal-only expression of *U2af1-rs1* in brain (11,18). However, as with *Blcap*, we found EST evidence (e.g. BG074660, BE137092, BU582903) for alternative *Commd1* transcripts (*Commd1_v2a, b, c*) originating from within or near the 5′-end of the intronic *U2af1-rs1* gene (Supplementary Material, Fig. S3A). Using a G/A SNP between the B6 and cast strains in the first exon of *Commd1_v2b*, we determined that this isoform is exclusively

paternally expressed (Supplementary Material, Fig. S3B). The *Commd1* microarray probe sets map to the second and third *Commd1* exons that are common to all isoforms (Supplementary Material, Fig. S3A). The fact that they detected preferential maternal expression suggests that paternal *Commd1* transcripts like *Commd1_v2a* are much less abundant than the maternally expressed *Commd1_v1a* that was assayed in reference (11), similar to the relative abundances of *Blcap_v1a* and *Blcap_v2a*.

DISCUSSION

Tissue- and promoter-specific imprinting of *Blcap*/*Blcap*

The *BLCAP*/*Blcap* locus generates transcripts from distinct promoters downstream (*BLCAP_V1*/*Blcap_v1*) and upstream (*BLCAP_V2*/*Blcap_v2*) of *NNAT*/*Nnat* (Fig. 1). We found *Blcap_v1a* to be preferentially expressed from maternally inherited alleles in brain but not other murine tissues, indicating brain-specific imprinting (Fig. 2A and Supplementary Material, Fig. S1). Similarly, *BLCAP_V1* transcripts are preferentially maternally expressed in human fetal brain (Fig. 5). In contrast, the *BLCAP_V2a*/*Blcap_v2a* isoforms are predominantly paternally expressed in brain (Figs 2C and 5). In mouse brain, *Blcap_v1a* is much more abundant than *Blcap_v2a* (Fig. 3B), explaining the overall dominance of *Blcap* transcripts from maternal alleles (microarray data and Fig. 4), which is also evident in human (Fig. 5). The transcriptional profile of *BLCAP*/*Blcap* is thus a complex combination of tissue-specific expression, promoters of different efficiencies and tissue- and promoter-specific imprinting.

This complexity is reminiscent of the *GRB10*/*Grb10* locus. In mouse, the 'major' *Grb10* promoter is active in a range of tissues but only on maternally inherited alleles (19), while distinct brain-specific promoters are utilized on only paternal alleles (20–23). In human, the 'major' *GRB10* promoter is active on both parental alleles (20,24,25). *BLCAP*/*Blcap* thus shares the promoter-specific expression of either predominantly the maternal or the paternal alleles (Figs 2A and C), but in contrast to *GRB10*/*Grb10*, this 'reciprocal' imprinting pattern occurs in the same tissue and is conserved in human (Fig. 5).

Previously, *Blcap* expression has been detected by qualitative methods in both parthenogenote and androgenote as well as in MatDp(dist2) and PatDp(dist2) mouse embryos (10). This is consistent with the contribution of non-brain tissues in which we found *Blcap_v1a* to be expressed biallelically (Supplementary Material, Fig. S1) and the incomplete silencing of the paternal allele of *Blcap_v1a* even in brain (Figs 2A and 3A). Similarly in human, a qualitative expression assay yielded biallelic results for *BLCAP* in various fetal tissues including brain (7). The brain-specific result is again probably due to the incomplete suppression of *BLCAP_V1* transcription from the paternal allele (Fig. 5).

Transcriptional interference hypothesis

The *Blcap*/*Nnat* locus is similar in many respects to the *Commd1*/*U2af1-rs1* locus (11,18). *Commd1_v1a* is preferentially maternally expressed, particularly in adult brain where the paternally expressed *U2af1-rs1* is abundant relative to earlier developmental stages and other tissues (11). *In situ* hybridizations showed *Commd1* and *U2af1-rs1* to be co-expressed widely throughout the brain and in the same cell types (11). In addition, paternally expressed anti-sense transcripts overlap the *Commd1_v1a* promoter region, are most abundant in brain and likely correspond to *U2af1-rs1* transcripts (11). Transcription of *U2af1-rs1* through the *Commd1_v1a* promoter was postulated to interfere with *Commd1_v1a* expression in *cis* where the degree of interference directly relates to *U2af1-rs1* expression levels (11). This transcriptional interference mechanism would explain the imprinted expression profile of *Commd1_v1a*.

Here, we have shown that specifically in brain, *Blcap_v1a*, like *Commd1_v1a*, is preferentially expressed from the maternal allele. *Nnat*, like *U2af1-rs1*, is highly expressed in brain compared to other tissues. *Nnat* expression is particularly low in the murine tissues in which we found *Blcap_v1a* to be biallelically expressed (Fig. 2B). A NeuroBlast (26) search, based on the *in situ* hybridization data for thousands of genes that compose the Allen Brain Atlas (27), found *Blcap* to have the most similar expression pattern in brain relative to *Nnat* (Supplementary Material, Table S2). This suggests that in brain, *Nnat* and *Blcap* are co-expressed in the same cell types. Our data on paternal allele-specific transcripts in the first intron of *Blcap_v1a* may reflect *Nnat* transcripts extending through the *Blcap_v1a* promoter region (Fig. 2D). Thus, the transcriptional interference mechanism proposed by Wang *et al*. (11) for *Commd1/U2af1-rs1* may also be acting at the *Blcap*/*Nnat* locus.

Alternative polyadenylation hypothesis

For the *H13*/*Mcts2* imprinted locus, we recently demonstrated parent-of-origin-specific *H13* polyA site selection (12). An *H13* intron contains the paternally expressed gene *Mcts2*. Alternative *H13* polyA sites upstream of *Mcts2* are preferentially utilized on the paternal allele. On the maternal allele, *H13* transcription proceeds through the inactive *Mcts2* to downstream polyA sites. The ICR of the locus is a CGI overlapping the *Mcts2* promoter that carries a maternal germ-line methylation mark. The organization of the *H13*/*Mcts2* locus thus is similar to *Blcap*/*Nnat*. The paternal allele-specific transcripts overlapping the first exon and extending into the intron of *Blcap_v1a* (Fig. 2D), instead of being generated by *Nnat*, may reflect the use of an alternative *Blcap* polyA site on specifically paternal alleles and preferentially in brain. This assumes that high transcriptional activity of *Nnat* can reduce the utilization of the canonical *Blcap* polyA site in favour of the alternative site. Like transcriptional interference, alternative polyA could explain the observed brain-specific preferential maternal expression of *Blcap_v1a*.

Possible implications of *BLCAP/NNAT* imprinting for carcinogenesis

Expression studies in various cancers have consistently found *BLCAP* to be absent or down-regulated relative to normal or less severe controls (Supplementary Material, Table S3). Reducing *BLCAP* expression by RNAi in osteosarcoma cells has been reported to increase cell growth and colony formation, alters the cell cycle and promotes cell proliferation (28).

In contrast, over-expression of *BLCAP* in HeLa and human tongue cancer cells has been shown to stimulate apoptosis (3,4).

Similar studies of *NNAT* include observations of down- as well as up-regulation in different cancers (Supplementary Material, Table S3). Several of these investigations assessed the DNA methylation state of the *NNAT* promoter and/or the effect of DNA de-methylation agents on the expression of *NNAT*, but none of the reports about elevated *NNAT* expression in cancer included information on its methylation state. De-methylation and reactivation of maternal *NNAT* may have occurred in these cases. Global as well as locus-specific hypomethylation, often in introns, has previously been observed in cancer (29,30).

In the context of the transcriptional interference model, this may be relevant to carcinogenesis in tissues like brain where *NNAT* is highly expressed. Reactivation of maternal *NNAT* would lead to an overall down-regulation of *BLCAP*, akin to our results for *Blcap* in *Dnmt3l*$^{-/+}$ mouse embryos (Fig. 3C). So, with respect to *BLCAP* expression levels, hypomethylation of *NNAT* would have an effect similar to hypermethylation and silencing of the *BLCAP* promoter.

NNAT and *BLCAP* have not been studied in concert in cancer biology. Some studies employed large-scale methods that implicitly generated limited data for both genes (31,32). Care needs to be taken when choosing polymorphisms for allele-specific profiling: *BLCAP* message is the target of RNA editing, particularly in brain, generating what appear to be A/G SNPs (33,34). We believe that a simultaneous allele-specific profiling of *NNAT* and *BLCAP* expression and chromatin modifications in tumours and cell lines would be insightful.

MATERIALS AND METHODS

Mouse samples

Tissues of B6, cast and inter-subspecies hybrids (B×C and C×B) were dissected, snap-frozen and stored at −80°C. The MatDp(dist2), PatDp(dist2) and non-UpDp control newborn mice were generated as described in reference (13). Briefly, these mice are the offspring of heterozygotes for the T(2:9)11H reciprocal translocation that have inherited the distal part of both homologous copies of Chr 2 from either the mother, MatDp(dist2), or the father, PatDp(dist2), due to a non-disjunction event. The non-UpDp controls were carriers of the T(2:9)11H translocation with an otherwise normal, that is, biparental and balanced genome. The generation of the 8.5 dpc Dnmt3l$^{-/+}$ embryos and normal litter mates is described in reference (14). RNA and DNA were extracted with the Qiagen RNeasy mini (Cat. No. 74104) and DNeasy tissue kits (Cat. No. 69504) following manufacturer protocols. cDNA was made with the Invitrogen Superscript First-Strand Synthesis System (Cat. No. 12371-019). Between 1 and 5 μg of total RNA, quantified with an Agilent 2100 BioAnalyzer, were used in a standard 50 μl oligo dT-primed reaction following the manufacturer protocol.

Human samples

The brain samples of fetuses 1 and 3 were obtained from the MRC-Wellcome Human Developmental Biology Resource. RNA and DNA were extracted with the Qiagen RNeasy mini (Cat. No. 74104) and DNeasy tissue kits (Cat. No. 69504) following manufacturer protocols. cDNA was synthesized using the Invitrogen Superscript First-Strand Synthesis System (Cat. No. 12371-019). For fetus F46, brain cDNA and maternal genomic DNA samples were collected under the guidelines of the Hammersmith and Queen Charlotte's and Chelsea Hospitals Trust Research Ethics Committee (Registration No. 2005/6028). Informed consent was collected from all subjects.

Expression microarrays

Two Affymetrix MOE 430 v2 expression microarrays were hybridized with probes produced from total RNA samples of the whole heads of a MatDp(dist2) and a PatDp(dist2) newborn mouse, respectively. Probe generation, array hybridization and analysis are described in references (16) and (17). The data can be viewed using WAMIDEX (https://atlas.genetics.kcl.ac.uk), the web interface to our collection of imprinting-related microarray data (16). The raw array data are available from GEO (GSE11789).

PCR

All reactions were performed using Abgene Reddymix (Cat. No. AB-0575/LD/A). Unless noted otherwise, total reaction volume was 10 μl, including 1 μl cDNA template and 0.5 μl mix of 20 μM forward and reverse primer. Primer sequences and cycling conditions are listed in Supplementary Material, Table S1. Primers were designed using Primer3Plus (35). For fetus F46, two rounds of PCR with nested primers were necessary to obtain enough product from brain cDNA for sequencing. Two microlitre of the first round PCR reaction were used as template in the second round.

DNA sequencing

2.5 μl of PCR reaction was treated with 1 μl USB Exosap-IT (Cat. No. 78200) in a 15 μl reaction to inactivate primers and unincorporated nucleotides. Depending on the concentration of the PCR product as estimated by gel electrophoresis using 1.2% agarose, 2.5 or 5 μl of the Exosap reaction were used as template in a 10 μl sequencing reaction together with 0.5–1.0 μl BigDye and 2 μl 5× sequencing buffer from the ABI BigDye v3.1 kit (Cat. No. 4337455) and 0.4 μl 20 μM primer. Primer sequences and cycling conditions are listed in Supplementary Material, Table S1. The products were precipitated with 300 mM sodium acetate in ethanol, collected by centrifugation, washed with 70% ethanol, resuspended and denatured in formamide and sequenced on an ABI 3730xl sequencer. Sequence reads were analysed with the Staden package (http://staden.sourceforge.net/) (36).

qRT–PCR

Custom TaqMan gene expression assays (primer-probe mixes) for *Blcap_v1a* and *v2a* were ordered from ABI (Cat. No. 4331348). One microlitre of cDNA template was diluted in 3.5 μl water and added to 0.5 μl primer-probe mix in 5 μl

ABI TaqMan Gene Expression Master Mix (Cat. No. 4370048). The reactions were performed on an ABI 7900ht Lightcycler and analysed using the ΔΔCt method with *Actb* as the endogenous control (37). The confidence intervals shown in Figure 3 are based on four replicate reactions per transcript and template. Primer and probe sequences and cycling conditions are listed in Supplementary Material, Table S1.

Northern hybridization

Two blots were generated in parallel from 10 μg per well of total RNA extracted from single MatDp(dist2), PatDp(dist2) or non-UpDp control newborn brains. Size estimates are based on a DNA ladder run in parallel. PCR primers and conditions for the generation of the templates for the ∼200 bp probes N1 and N2 shown in Figure 1B are given in Supplementary Material, Table S1. Twenty microlitre of template PCR product was purified by gel electrophoresis in 1.2% low melting point agarose and gel-extracted with the Qiagen QiaEx II kit (Cat. No. 20021). Five microlitre (∼25 ng) of purified template was used to make αdCT ^{32}P-labelled probe with the NEBlot kit (Cat. No. N1500S) in a standard 50 μl reaction, which was purified with a Roche mini Quick Spin DNA Column (Cat. No. 11814419001). The probe in 10 ml Sigma PerfectHyb solution (Cat. No. H7033-125ML) was incubated with the respective blot (pre-hybridized with 10 ml PerfectHyb for 2hrs) at 65°C overnight. Blots were washed at 65°C for 20 min in 2% SSC, 0.5% SDS and for 40 min in 0.5% SSC, 0.5% SDS. The blot probed with N1 (last *Blcap* exon) was exposed to phosphor screen for 15 h. The exposure time for the N2 blot (*Blcap_v2a* exon 1) was 84 h. The phosphor screen was scanned with an Amersham Typhoon 9200 Variable Mode Imager at 50 μm resolution.

Bisulfite mutagenesis DNA methylation assay

Genomic DNA extracted from 7.75 dpc *Dnmt3l*$^{-/+}$ and wild-type visceral yolk sac (VYS) tissue was bisulfite-converted using the Zymo Research EZ DNA Methylation-Direct Kit (Cat. No. D5020) according to the manufacturer's protocol (∼500 ng input DNA per reaction). Genomic DNA of 8.5 dpc *Dnmt3l*$^{-/+}$ embryos was converted as described (12). Four microlitre of converted DNA were used for each PCR with Thermoprime *Taq* DNA polymerase (Thermo Scientific Cat. No. AB-0301) according to the manufacturer's protocol, adjusted for a 20 μl reaction volume and the addition of 4 μl 5M Betaine (Sigma Cat. No. B0300). The products were directly sequenced as well as cloned and sequenced using the pGEM-T Easy vector (Promega Cat. No. A1360) and DH5α competent cells (Invitrogen). Primers and cycling conditions are provided in Supplementary Material, Table S1. Primers were designed using BiSearch (38). 'Beads-on-a-string' diagrams were produced with BiQ Analyzer (39).

SUPPLEMENTARY MATERIAL

Supplementary Material is available at *HMG* Online.

ACKNOWLEDGEMENTS

We thank Colin Beechey and Jo Peters for the MatDp(dist2) and PatDp(dist2) material, and Deborah Bourc'his and Timothy Bestor for the Dnmt3l$^{-/+}$ material.

Conflict of Interest statement. The authors declare that there are no conflicts of interest with regard to the work presented in this article.

FUNDING

The Wellcome Trust to R.J.O.; Biotechnology and Biological Sciences Research Council to R.J.O.; European Molecular Biology Organisation to R.S. Funding to pay the Open Access charges was provided by the Wellcome Trust.

REFERENCES

1. Gromova, I., Gromov, P. and Celis, J.E. (1999) Identification of true differentially expressed mRNAs in a pair of human bladder transitional cell carcinomas using an improved differential display procedure. *Electrophoresis*, **20**, 241–248.
2. Rae, F.K., Stephenson, S.A., Nicol, D.L. and Clements, J.A. (2000) Novel association of a diverse range of genes with renal cell carcinoma as identified by differential display. *Int. J. Cancer*, **88**, 726–732.
3. Zuo, Z., Zhao, M., Liu, J., Gao, G. and Wu, X. (2006) Functional analysis of bladder cancer-related protein gene: a putative cervical cancer tumor suppressor gene in cervical carcinoma. *Tumour Biol.*, **27**, 221–226.
4. Yao, J., Duan, L., Fan, M., Yuan, J. and Wu, X. (2007) Overexpression of BLCAP induces S phase arrest and apoptosis independent of p53 and NF-B in human tongue carcinoma: BLCAP overexpression induces S phase arrest and apoptosis. *Mol. Cell. Biochem.*, **297**, 81–92.
5. Su, A.I., Wiltshire, T., Batalov, S., Lapp, H., Ching, K.A., Block, D., Zhang, J., Soden, R., Hayakawa, M., Kreiman, G. *et al.* (2004) A gene atlas of the mouse and human protein-encoding transcriptomes. *Proc. Natl Acad. Sci. USA*, **101**, 6062–6067.
6. Gromova, I., Gromov, P. and Celis, J.E. (2002) bc10: a novel human bladder cancer-associated protein with a conserved genomic structure downregulated in invasive cancer. *Int. J. Cancer*, **98**, 539–546.
7. Evans, H.K., Wylie, A.A., Murphy, S.K. and Jirtle, R.L. (2001) The neuronatin gene resides in a 'micro-imprinted' domain on human chromosome 20q11.2. *Genomics*, **77**, 99–104.
8. Kagitani, F., Kuroiwa, Y., Wakana, S., Shiroishi, T., Miyoshi, N., Kobayashi, S., Nishida, M., Kohda, T., Kaneko-Ishino, T. and Ishino, F. (1997) Peg5/Neuronatin is an imprinted gene located on sub-distal chromosome 2 in the mouse. *Nucleic Acids Res.*, **25**, 3428–3432.
9. Kikyo, N., Williamson, C.M., John, R.M., Barton, S.C., Beechey, C.V., Ball, S.T., Cattanach, B.M., Surani, M.A. and Peters, J. (1997) Genetic and functional analysis of Neuronatin in mice with maternal or paternal duplication of distal chromosome 2. *Dev. Biol.*, **190**, 66–77.
10. John, R.M., Aparicio, S.A., Ainscough, J.F., Arney, K.L., Khosla, S., Hawker, K., Hilton, K.J., Barton, S.C. and Surani, M.A. (2001) Imprinted expression of neuronatin from modified BAC transgenes reveals regulation by distinct and distant enhancers. *Dev. Biol.*, **236**, 387–399.
11. Wang, Y., Joh, K., Masuko, S., Yatsuki, H., Soejima, H., Nabetani, A., Beechey, C.V., Okinami, S. and Mukai, T. (2004) The mouse Murr1 gene is imprinted in the adult brain, presumably due to transcriptional interference by the antisense-oriented U2af1-rs1 gene. *Mol. Cell. Biol.*, **24**, 270–279.
12. Wood, A.J., Schulz, R., Woodfine, K., Koltowska, K., Beechey, C.V., Peters, J., Bourc'his, D. and Oakey, R.J. (2008) Regulation of alternative polyadenylation by genomic imprinting. *Genes Dev.*, **22**, 1141–1146.
13. Cattanach, B.M. and Beechey, C.V. (1997) Genomic imprinting in the mouse: possible final analysis. Reik, W. and Surani, M.A. (eds), *Genomic Imprinting: Frontiers in Molecular Biology.* Vol. **18**. IRL Press, New York, Oxford, Tokyo, pp. 118–145.

14. Bourc'his, D., Xu, G.L., Lin, C.S., Bollman, B. and Bestor, T.H. (2001) Dnmt3L and the establishment of maternal genomic imprints. *Science*, **294**, 2536–2539.
15. Bourc'his, D. and Proudhon, C. (2007) Sexual dimorphism in parental imprint ontogeny and contribution to embryonic development. *Mol. Cell. Endocrinol.*, **282**, 87–94.
16. Schulz, R., Woodfine, K., Menheniott, T.R., Bourc'his, D., Bestor, T. and Oakey, R.J. (2008) WAMIDEX: a web atlas of murine genomic imprinting and differential expression. *Epigenetics*, **3**, 89–96.
17. Schulz, R., Menheniott, T.R., Woodfine, K., Wood, A.J., Choi, J.D. and Oakey, R.J. (2006) Chromosome-wide identification of novel imprinted genes using microarrays and uniparental disomies. *Nucleic Acids Res.*, **34**, e88.
18. Hatada, I., Sugama, T. and Mukai, T. (1993) A new imprinted gene cloned by a methylation-sensitive genome scanning method. *Nucleic Acids Res.*, **21**, 5577–5582.
19. Miyoshi, N., Kuroiwa, Y., Kohda, T., Shitara, H., Yonekawa, H., Kawabe, T., Hasegawa, H., Barton, S.C., Surani, M.A., Kaneko-Ishino, T. and Ishino, F. (1998) Identification of the Meg1/Grb10 imprinted gene on mouse proximal chromosome 11, a candidate for the Silver-Russell syndrome gene. *Proc. Natl Acad. Sci. USA*, **95**, 1102–1107.
20. Hikichi, T., Kohda, T., Kaneko-Ishino, T. and Ishino, F. (2003) Imprinting regulation of the murine Meg1/Grb10 and human GRB10 genes; roles of brain-specific promoters and mouse-specific CTCF-binding sites. *Nucleic Acids Res.*, **31**, 1398–1406.
21. Arnaud, P., Monk, D., Hitchins, M., Gordon, E., Dean, W., Beechey, C.V., Peters, J., Craigen, W., Preece, M., Stanier, P. *et al.* (2003) Conserved methylation imprints in the human and mouse GRB10 genes with divergent allelic expression suggests differential reading of the same mark. *Hum. Mol. Genet.*, **12**, 1005–1019.
22. Yamasaki-Ishizaki, Y., Kayashima, T., Mapendano, C.K., Soejima, H., Ohta, T., Masuzaki, H., Kinoshita, A., Urano, T., Yoshiura, K., Matsumoto, N. *et al.* (2007) Role of DNA methylation and histone H3 lysine 27 methylation in tissue-specific imprinting of mouse Grb10. *Mol. Cell. Biol.*, **27**, 732–742.
23. Sanz, L.A., Chamberlain, S., Sabourin, J.C., Henckel, A., Magnuson, T., Hugnot, J.P., Feil, R. and Arnaud, P. (2008) A mono-allelic bivalent chromatin domain controls tissue-specific imprinting at Grb10. *EMBO J.*, Advance online publication on Jul 24.
24. Blagitko, N., Mergenthaler, S., Schulz, U., Wollmann, H.A., Craigen, W., Eggermann, T., Ropers, H.H. and Kalscheuer, V.M. (2000) Human GRB10 is imprinted and expressed from the paternal and maternal allele in a highly tissue- and isoform-specific fashion. *Hum. Mol. Genet.*, **9**, 1587–1595.
25. Hitchins, M.P., Monk, D., Bell, G.M., Ali, Z., Preece, M.A., Stanier, P. and Moore, G.E. (2001) Maternal repression of the human GRB10 gene in the developing central nervous system; evaluation of the role for GRB10 in Silver-Russell syndrome. *Eur. J. Hum. Genet.*, **9**, 82–90.
26. Lau, C., Ng, L., Thompson, C., Pathak, S., Kuan, L., Jones, A. and Hawrylycz, M. (2008) Exploration and visualization of gene expression with neuroanatomy in the adult mouse brain. *BMC Bioinformatics*, **9**, 153.
27. Lein, E.S., Hawrylycz, M.J., Ao, N., Ayres, M., Bensinger, A., Bernard, A., Boe, A.F., Boguski, M.S., Brockway, K.S., Byrnes, E.J. *et al.* (2007) Genome-wide atlas of gene expression in the adult mouse brain. *Nature*, **445**, 168–176.
28. Fan, D.G., Fan, Q.Y., Zhang, H.Z., Zhang, Y.H. and Liu, Y.Y. (2004) A prospective genetic therapy study of extremity saving operations: the regulatory function of gene BLCAP in the development of human osteosarcoma. *Chin. J. Clin. Rehabil.*, **8**, 982–983.
29. Kanai, Y. and Hirohashi, S. (2007) Alterations of DNA methylation associated with abnormalities of DNA methyltransferases in human cancers during transition from a precancerous to a malignant state. *Carcinogenesis*, **28**, 2434–2442.
30. Wilson, A.S., Power, B.E. and Molloy, P.L. (2007) DNA hypomethylation and human diseases. *Biochim. Biophys. Acta*, **1775**, 138–162.
31. Dekel, B., Metsuyanim, S., Schmidt-Ott, K.M., Fridman, E., Jacob-Hirsch, J., Simon, A., Pinthus, J., Mor, Y., Barasch, J., Amariglio, N. *et al.* (2006) Multiple imprinted and stemness genes provide a link between normal and tumor progenitor cells of the developing human kidney. *Cancer Res.*, **66**, 6040–6049.
32. Keshet, I., Schlesinger, Y., Farkash, S., Rand, E., Hecht, M., Segal, E., Pikarski, E., Young, R.A., Niveleau, A., Cedar, H. and Simon, I. (2006) Evidence for an instructive mechanism of de novo methylation in cancer cells. *Nat. Genet.*, **38**, 149–153.
33. Clutterbuck, D.R., Leroy, A., O'Connell, M.A. and Semple, C.A. (2005) A bioinformatic screen for novel A-I RNA editing sites reveals recoding editing in BC10. *Bioinformatics*, **21**, 2590–2595.
34. Paz, N., Levanon, E.Y., Amariglio, N., Heimberger, A.B., Ram, Z., Constantini, S., Barbash, Z.S., Adamsky, K., Safran, M., Hirschberg, A. *et al.* (2007) Altered adenosine-to-inosine RNA editing in human cancer. *Genome Res.*, **17**, 1586–1595.
35. Untergasser, A., Nijveen, H., Rao, X., Bisseling, T., Geurts, R. and Leunissen, J.A. (2007) Primer3Plus, an enhanced web interface to Primer3. *Nucleic Acids Res.*, **35**, W71–W74.
36. Staden, R., Beal, K.F. and Bonfield, J.K. (2000) The Staden package, 1998. *Methods Mol. Biol.*, **132**, 115–130.
37. Pfaffl, M.W. (2001) A new mathematical model for relative quantification in real-time RT–PCR. *Nucleic Acids Res.*, **29**, e45.
38. Arányi, T., Váradi, A., Simon, I. and Tusnády, G.E. (2006) The BiSearch web server. *BMC Bioinformatics*, **7**, 431.
39. Bock, C., Reither, S., Mikeska, T., Paulsen, M., Walter, J. and Lengauer, T. (2005) BiQ Analyzer: visualization and quality control for DNA methylation data from bisulfite sequencing. *Bioinformatics*, **21**, 4067–4068.
40. Kent, J.W., Sugnet, C.W., Furey, T.S., Roskin, K.M., Pringle, T.H., Zahler, A.M. and Haussler, D. (2002) The human genome browser at UCSC. *Genome Res.*, **12**, 996–1006.